Carbonylation of four-membered ruthenium and osmium metallacycles incorporating an orthometallated phenolic function: New acylruthenium and arylosmium complexes

Bikash Kumar Panda [a], Animesh Chakravorty [a,b,*]

[a] *Department of Inorganic Chemistry, Indian Association for the Cultivation of Science, Jadavpur, Kolkata 700 032, India*
[b] *Jawaharlal Nehru Centre for Advanced Scientific Research, Bangalore 560 064, India*

Abstract

The solution reaction of $Ru(QL^1)(PPh_3)_2(CO)Cl$ (**3**) and $Os(QL^1)(PPh_3)_2(CO)Br$ (**4**) with carbon monoxide at one atmosphere pressure has respectively afforded the orange acylruthenium system $Ru(QL^2)(PPh_3)_2(CO)Cl$ (**5**) and the yellow arylosmium dicarbonyl system $Os(QL^3)(PPh_3)_2(CO)_2Br$ (**6**) in excellent yields. (QL^1 is C_6H_2O-2-$CHNHC_6H_4Q(p)$-3-Me-5, QL^2 is $C_6H_2(CO-1)O$-2-$CHNHC_6H_4Q(p)$-3-Me-5 and QL^3 is C_6H_2OH-2-$CHNC_6H_4Q(p)$-3-Me-5 and Q is Me, OMe and Cl.) It is proposed that in the case of **3** a dicarbonyl complex similar to **6** is formed as an intermediate which rapidly undergoes aryl migration with concomitant phenolato coordination furnishing **5**. The stability of **6** is consistent with the greatly diminished ability of osmium in promotion of migratory reactions. In the reaction **4** → **6** the Os–O(phenolato) bond is cleaved and the Schiff base moiety undergoes iminium-phenolato → imine-phenol tautomerization. The observed *cis* geometry of **6** may arise by a concerted route involving edge displacement of the halide ligand. The crystal and molecular structure of **5**(Q = Cl) has revealed the presence of a distorted octahedral RuC_2P_2OCl coordination sphere and a highly planar acyl chelate ring characterized by a Ru–C distance of 2.013(4) Å. In the hydrogen bonded zwitterionic iminium-phenolato ring the N ⋯ O distance is 2.561(6) Å. The acyl complexes of type **5** display an MLCT band near 500 nm which is absent in **6**. The Schiff base C=N stretch in **5** ($\sim$1630 cm^{-1}) is significantly higher than that in **6** ($\sim$1600 cm^{-1}) which displays two strong C≡O stretches near 2020 and 1940 cm^{-1} (*cis*-$Os(CO)_2$ configuration). A single ^{31}P NMR signal occurs in both **5** and **6** near 37 and −6 ppm, respectively (*trans*-$M(PPh_3)_2$ configuration). The voltammetric reduction potentials of the M^{III}/M^{II} couple is observed near 1.0 and 0.8 V vs. SCE in **5** and **6**, respectively. Both are significantly higher than those in parent complexes (**3** and **4**) due to stabilization of the bivalent state upon carbonylation.
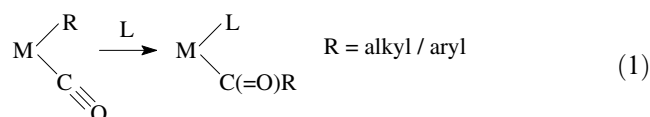© 2005 Elsevier B.V. All rights reserved.

Keywords: Acylruthenium chelates; Dicarbonyl arylosmium complexes; Migratory aryl insertion

1. Introduction

Metal mediated migratory insertion reactions of the type stated in Eq. (1) has been of abiding interest in transition metal organometallic chemistry [1,2]. In ruthenium chemistry it has been observed in mononuclear dicarbonyl species of type

$$M \overset{R}{\underset{C\equiv O}{\Big\langle}} \quad \overset{L}{\longrightarrow} \quad M \overset{L}{\underset{C(=O)R}{\Big\langle}} \qquad R = \text{alkyl / aryl} \tag{1}$$

$Ru(CO)_2X(R)(D)_2$ (X = halide, D = tertiary phosphines) [3,4], hydridocarbonyls and hydridodienes [5],

alkyl and aryl systems [6], metallacycles [7,8], and binuclear species [9,10].

In the present work we scrutinize the reaction of the four-membered metallacycle **1** with carbon monoxide via product isolation and characterization. Several considerations encouraged us in this endeavour. First, **1** is known to be reactive towards small unsaturates like alkynes [11] and isonitriles [12] as well as towards certain other donors [13–15]. Second, **1** is generated *via* decarbonylative metallation of formylphenols [16,17] and its carbonylation would be an interesting case of reaction reversal. Third, structural
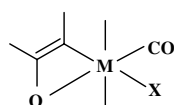
1, M = Ru, X = Cl
2, M = Os, X = Br

characterization of a inserted product would be of interest as accurate structures of very few ruthenium acyls are known [3c,9,12]. Last, a comparative study of the carbonylation behaviour of **1** with that of the osmium analogue **2** would be of interest since known instances of such comparisons are rare [4b,8].

The metallacycle **1** has indeed been found to undergo a smooth insertion reaction affording acyl phenolato species. The reaction of **2** did not lead to insertion and afforded only an unreactive *cis*-dicarbonyl complex which has, however, provided a possible model for the reaction intermediate in the carbonylation of **1**. The new organometallics have been isolated in the pure state and have been spectrally and electrochemically characterized. The structure of an acylruthenium system is reported.

2. Results and discussion

2.1. Parent complexes and their carbonylation

The substrates [16,17] incorporating the metallacycles **1** and **2** are $Ru(QL^1)(PPh_3)_2(CO)Cl$ (**3**) and $Os(QL^1)(PPh_3)_2(CO)Br$ (**4**). The Q substituents used are Me, OMe and Cl. Specific compounds will be identified by putting the Q group in parenthesis as in **3**(Me) meaning **3** having Q = Me.

Upon exposing a stirred dichloromethane solution of **3** to carbon monoxide at one atmosphere pressure for a few hours, the orange acylruthenium system $Ru(QL^2)(PPh_3)_2(CO)Cl$ (**5**) is afforded in excellent yields. A similar treatment of **4** furnished the yellow coloured dicarbonyl family $Os(QL^3)(PPh_3)_2(CO)_2Br$ (**6**). Here no acyl complex could be isolated or identified in the reaction mixture. Both reactions, Eqs. (2) and (3), involve the addition of one CO molecule but the final products are

3, M = Ru, X = Cl
4, M = Os, X = Br

5
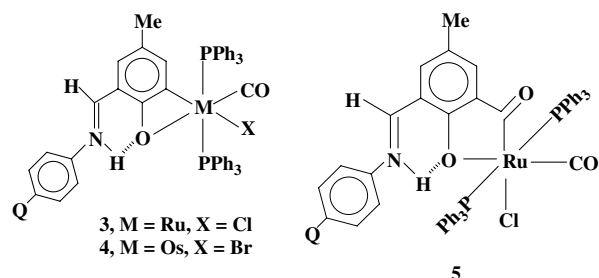
dramatically different. In Eq. (2) we observed migratory insertion and in Eq. (3) mere CO

$$3 + CO \rightarrow 5 \qquad (2)$$

$$4 + CO \rightarrow 6 \qquad (3)$$

ligation at the expense of Os–O(phenolato) bond cleavage. A consequence of this cleavage is the tautomerization of the Schiff base moiety from coordinated iminium-phenolato from (as in **3–5**) to the pendant imine-phenol form (as in **6**).

6
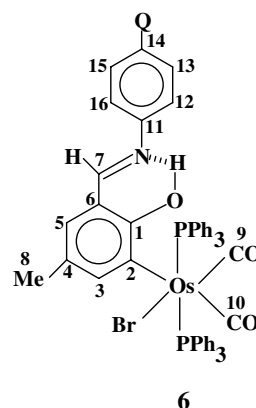
2.2. Reaction model

The facile formation of the dicarbonyl complex **6** in the case of osmium prompts us to propose that the reaction of Eq. (2) proceeds via the intermediacy of a similar ruthenium complex stylized as **7** (PPh_3 ligands not shown) which can afford the acyl complex **5** via straightforward nucleophilic aryl migration with concomitant phenolato coordination, Eq. (4). The fact that under ambient condition **7** is highly reactive and **6** is not is qualitatively consistent with the greatly diminished ability of osmium

7   5

$$(4)$$
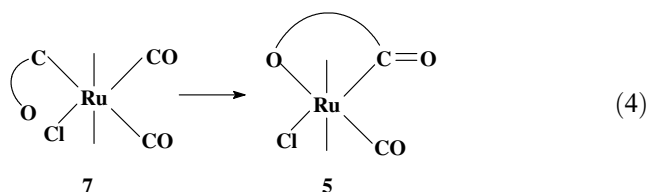
(compared to ruthenium) in promoting migratory acyl formation [4b,8]. It is plausible that the observed *cis* geometry of **6** (and **7**, by inference) arises via a concerted route wherein carbon monoxide attack on **4** (or **3**) is associated with edge displacement [18] of the halide ligand, Eq. (5) as in some other reactions of **4** and **3** [11b,13a].

$$\text{(5)}$$
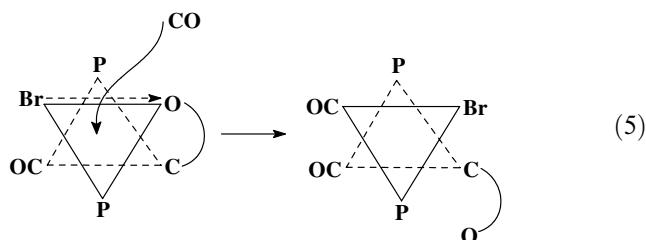
Finally we note that the formation of the parent complex **3** [16,17] from Ru(PPh$_3$)$_3$Cl$_2$ and the Schiff monobase of 4-methyl-2,6-diformyl-phenol probably proceeds via oxidative addition [17] of the aldehyde function generating the moiety **8** which then undergoes aryl migration with C–CO bond scission, Ru–C(aryl) bond formation and reductive proton elimination leading to the metallacycle **3**. With the availability of an extra carbon monoxide ligand the above noted aryl migration protocol is essentially reversed and a C–CO bond is formed leading the transformation of Eq. (2).

8
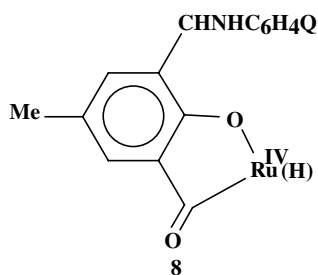
2.3. Spectral features

The compositions of the complexes were confirmed by positive ion electrospray mass spectra. Representative maximum molecular ion peaks (*m/z*) are: **5** (OMe), 958.05 (formula weight, 957.4) and **6** (Cl), 1096.5 (fw, 1095.43). The molecular ion mass corresponds to [M + H]$^+$. In every case the observed isotopic distribution pattern in the molecular ion peak fitted excellently with the simulated pattern. All the complexes systematically displayed a peak corresponding to halide loss.

The acyl family **5** displays (Table 1) a characteristic allowed band near 500 nm which is assigned to $t_{2g} \rightarrow \pi^*$ MLCT within the chelated zwitterionic iminium-phenolato function **9** as in the precursor species **3** [16,17] and related derivatives [11,12]. In contrast

9
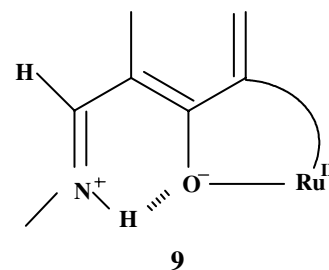
the dicarbonyl system **6** in which the Schiff base acts simply as a monocoordinated aryl ligand, there is no absorption band above ∼380 nm (Table 1).

In **5** a broad and strong IR band near 1630 cm^{-1} (Table 1) is believed to incorporate both the Schiff base C=N and C=O(acyl) stretches. The relatively high frequency for the C=N stretch is consistent with the protonation of the nitrogen atom in the iminium-phenolato function [11,12,17,19,20]. In contrast the C=N stretch of the imine-phenol moiety in **6** occurs at lower frequency, ∼1600 cm^{-1} (Table 1). Species of type **6** displays two strong C≡O stretches near 2020 and 1940 cm^{-1} characterizing the *cis*-Os(CO)$_2$ configuration [21]. The N$^+$–H stretch in **5** occurs near 3440 cm^{-1}.

The complexes generally show well-resolved ^{1}H NMR lines. The iminium N$^+$–H signal in **5** occur near 15 ppm and is split into a doublet due to *trans* coupling with the azomethine proton (∼12 Hz). In **6** the O–H resonance is observed as a sharp feature near 13 ppm as in related imine-phenol systems [13a,14b]. The complexes uniformly display a single ^{31}P NMR signal for the two phosphine ligands implicating *trans*-M(PPh$_3$)$_2$ configuration. The resonances occur near 37 and −6 ppm in **5** and **6**, respectively (Table 2).

2.4. Metal redox

The complexes exhibit a quasireversible one-electron cyclic voltammetric response in dichloromethane solution. The response is assigned to metal redox (M^{III}/M^{II}) and the reduction potentials are collected in Table 2. It is instructive to compare these with those of the parent complexes −0.7 V in **3** [17] and 0.6 V in **4** [17]. Formation of the five-membered acyl phenolato chelate ring in going from **3** to **5** stabilizes the bivalent state in the redox sense as reflected in the higher reduction potentials. Substitution of the Os–O(phenolato) bond by an Os–CO bond is going from **4** to **6** stabilizes the bivalent state via increased back-bonding resulting in higher reduction potentials. In both families the $E_{1/2}$ values follow the Hammett order of Q: OMe < Me < Cl.

2.5. Structure

The X-ray structure of **5** (Cl) has been determined. A molecular view is shown in Fig. 1 and selected bond

Table 1
UV–vis[a] and IR[b] spectral data

Compound	λ_{max}, nm (ε[c], M^{-1} cm^{-1})	$\nu_{C\equiv O}$	$\nu_{C=N}$ and $\nu_{C=O(acyl)}$	ν_{N-H}^{+}
5(Me)	341(9058), 497(7310)	1925	1633	3436
5(OMe)	353(11507), 501(10835)	1925	1631	3436
5(Cl)	342(11619), 503(8330)	1930	1633	3447
6(Me)	323(28860), 378(12340)	2016, 1936	1592	–
6(OMe)	331(25460), 374(14620)	2016, 1930	1607	–
6(Cl)	321(21790), 375(10900)	2026, 1960	1607	–

[a] Solvent is dichloromethane.
[b] In KBr disk.
[c] Extinction coefficient.

Table 2
Cyclic voltammetric reduction potentials[a] and ^{31}P NMR data

Complexes	$E_{1/2}$[b], M(III)/M(II), (ΔE_p, mV)	δ (ppm)
5(Me)	0.99 (152)	36.8
5(OMe)	0.96 (158)	36.6
5(Cl)	1.11 (200)	37.1
6(Me)	0.82 (116)	−6.2
6(OMe)	0.79 (175)	−6.3
6(Cl)	0.87 (143)	−6.3

[a] Solvent is dichloromethane.
[b] $E_{1/2} = 1/2(E_{pa} + E_{pc})$, $\Delta E_p = E_{pa} - E_{pc}$ where E_{pa} and E_{pc} are anodic and cathodic peak potentials respectively.

parameters are listed in Table 3. In the distorted octahedral RuC_2P_2OCl coordination sphere the RuC_2OCl fragment constitute a nearly perfect equatorial plane (mean deviation, 0.007 Å), the P1–Ru–P2 axis being approximately linear with an angle of 176.42(4)° at the metal. The acyl chelate ring Ru, C1, C2, C8 and O2 is highly planar (mean deviation, 0.006 Å) and indeed the $Ru(ClL^2)$ fragment excluding the chlorophenyl group is a good plane (mean deviation, 0.03 Å) which makes a dihedral angle of 23.4° with the pendant chlorophenyl plane.
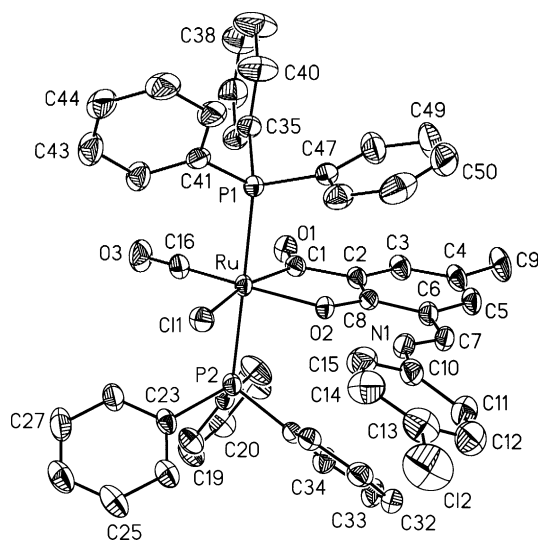
Structurally characterized acylruthenium species are relatively few. The Ru–C(acyl) and acyl C=O distances in **5** (Cl) are 2.013(4) and 1.226(5) Å, respectively. In the reported structurally characterized species these lengths have been found to occur in the ranges 1.98–2.15 and 1.20–1.34 Å, respectively [3c,6a,6b,6c,9,12]. The two Ru–P distances, 2.383(1) and 2.401(1) Å lie within the expected range [11–17] 2.40 ± 0.05 Å in *trans*-Ru^{II}(PPh$_3$)$_2$ species. The Ru–Cl length 2.558(1) Å is longer than usual presumably due to the *trans* influence of the coordinated acyl function.

In the hydrogen bonded zwitterionic iminium-phenolato ring, the N $\cdots$ O distance 2.561(6) Å is shorter than that in the precursor complex **3** (Me) [16b] (2.665(12) Å). The iminium hydrogen was directly observable in difference Fourier maps, the N$^+$–H and H $\cdots$ O distances are approximately 0.9 and 1.8 Å, respectively.

The type **6** complexes did not afford single crystal but their gross structure and geometry is convincingly proven by IR (*cis*-Os(CO)$_2$), ^{31}P NMR (*trans*-Os(PPh$_3$)$_2$), ^{1}H NMR (imine-phenol tautomeric state) UV–vis spectra (lack of metal chelation) and metal reduction potential (extra Os–CO back-bonding).

3. Experimental

3.1. Materials

The compounds Ru(PPh$_3$)$_3$Cl$_2$ [22], Os(PPh$_3$)$_3$Br$_2$ [23] and M(QL^1)(PPh$_3$)$_2$(CO)X [16,17] were prepared by reported methods. Pure carbon monoxide was delivered from a cylinder through gauges. The purification of dichloromethane and the preparation of tetraethylammonium perchlorate (TEAP) for electrochemical work were done as described in previous work [24a]. All other chemicals and solvents were of analytical grade and were used as received.

3.2. Physical measurements

Electronic, IR and mass spectra were recorded with Shimadzu UV-1601 PC spectrophotometer,

Fig. 1. Perspective view and atom-labelling scheme for Ru(ClL^2)(PPh$_3$)$_2$(CO)Cl, **5**(Cl).

Table 3
Selected bond distances (Å) and bond angles (°) for Ru(ClL^2)(PPh$_3$)$_2$(CO)Cl, **5**(Cl)

Bond distances			
Ru–P1	2.383(1)	C1–O1	1.226(5)
Ru–P2	2.401(1)	C16–O3	1.152(5)
Ru–C1	2.013(4)	C7–N1	1.299(6)
Ru–Cl6	1.821(5)	N1–C10	1.410(6)
Ru–O2	2.121(3)	N1···O2	2.561(6)
Ru–Cl1	2.558(1)	O2–C8	1.307(5)
Bond angles			
P1–Ru–P2	176.42(4)	P2–Ru–Cl1	86.80(4)
P1–Ru–C1	89.43(13)	Ru–Cl6–O3	178.2(4)
P1–Ru–O2	88.78(8)	O1–C1–Ru	132.2(3)
P1–Ru–Cl6	91.6(2)	O2–Ru–Cl1	80.75(8)
P1–Ru–Cl1	89.64(4)	O2–C8–Ru	112.1(3)
P2–Ru–C1	93.88(13)	C2–C1–Ru	109.6(3)
P2–Ru–O2	90.30(8)	O1–C1–Ru	132.2(3)
P2–Ru–Cl6	89.5(2)	C7–N1–C10	129.2(4)
O2–C8–C2	119.6(4)	N1–C7–C6	121.6(4)

Perkin–Elmer 783 IR spectrometer and Micromass Q-TOF mass spectrometer, respectively. A Bruker 300 MHz FT NMR spectrometer was used to record ^{1}H NMR spectra (Me$_4$Si internal standard). The numbering scheme used for ^{1}H NMR is the same as in crystallography in case of **5** and as in the drawing in the case of **6**. Spin–spin structures are abbreviated as: s, singlet; d, doublet; t, triplet; m, multiplet. ^{31}P NMR spectra were recorded with the help of a Varian 300 MHz spectrometer using H$_3$PO$_4$ as standard. Microanalyzes (C, H, N) were done using a Perkin–Elmer 240C elemental analyzer. All electrochemical measurement were done under a nitrogen atmosphere in dichloromethane solution using a model 620A electrochemical analyzer of CH Instruments. The supporting electrolyte was tetraethylammonium perchlorate and the reported potentials are referenced to the saturated calomel electrode (SCE).

3.3. Synthesis of the complexes, [Ru(QL^2)(PPh$_3$)$_2$(CO)Cl] (5)

The [Ru(QL^2)(PPh$_3$)$_2$(CO)Cl], (**5**) complexes were synthesized in excellent yield (~90%) by reacting Ru(QL^1)(PPh$_3$)$_2$(CO)Cl (**3**) with carbon monoxide. Details of a representative case are given below.

3.3.1. [Ru(MeL^2)(PPh$_3$)$_2$(CO) Cl], (5(Me))

One hundred milligrams (0.109 mmol) of Ru (MeL^1)(PPh$_3$)$_2$(CO)Cl was taken in a round bottom flask and 20 ml of dichloromethane was added. Initially dinitrogen gas was allowed to pass through the solution for 15 min followed by CO (1 atm, supplied from a cylinder) for 10 min. The solution was left under CO atmosphere for 12 h with constant stirring. The solution colour changed from violet to orange. After that the solvent was evaporated under reduced pressure when a orange

solid mass was obtained which was dissolved in a minimum volume of dichloromethane. Petroleum ether (boiling point 60–80 °C) was then added to precipitate the complex, which was filtered off and washed thoroughly by petroleum ether, affording a crystalline solid. It was dried in vacuo. Yield: 92 mg (89%). Anal. Found: C, 67.70; H, 4.76; N, 1.43%. Calc. for C$_{53}$H$_{44}$NO$_3$P$_2$ClRu: C, 67.62; H, 4.71; N, 1.49. MS (ES$^+$, CH$_2$Cl$_2$, *m/z*): 941.91(M + H)$^+$, 906.36 (M − Cl)$^+$. ^{1}H NMR (CDCl$_3$,δ): 7.84 (d, 1H, H(7), J_{HH} 12.5), 14.79 (d, 1H, N$^+$–H, J_{HH} 12.0), 6.65 (s, 1H, H(3)), 7.07 (s, 1H, H(5)), 2.10 and 2.39 (2s, 6H, 2CH$_3$), 7.15–7.67 (m, 34H, 2PPh$_3$, H(11), H(12), H(14) and H(15), arom).

3.3.2. [Ru(MeOL^2)(PPh$_3$)$_2$(CO)Cl], (5(OMe))

One hundred milligrams (0.107 mmol) Ru (MeOL^1)(PPh$_3$)$_2$(CO)Cl was employed. Yield: 95 mg (92%). Anal. Found: C, 66.55; H, 4.58; N, 1.43%. Calc. for C$_{53}$H$_{44}$NO$_4$P$_2$ClRu: C, 66.49; H, 4.63; N, 1.46. MS (ES$^+$, CH$_2$Cl$_2$, *m/z*): 958.05 (M + H)$^+$, 922.07 (M − Cl)$^+$. ^{1}H NMR (CDCl$_3$, δ): 7.78 (d, 1H, H(7), J_{HH} 12.3), 15.01 (d, 1H, N$^+$–H, J_{HH} 12.1), 6.64 (s, 1H, H(3)), 6.91 (s, 1H, H(5)), 2.09 (s, 3H, CH$_3$), 3.83 (s, 3H, OCH$_3$), 7.13–7.66 (m, 34H, 2PPh$_3$, H(11), H(12), H(14) and H(15), arom).

3.3.3. [Ru(ClL^2)(PPh$_3$)$_2$(CO)Cl], (5(Cl))

One hundred milligrams (0.107 mmol) of Ru(ClL^1)(PPh$_3$)$_2$(CO)Cl was employed. Yield: 90 mg (87%). Anal. Found: C, 64.89; H, 4.27; N, 1.52%. Calc. for C$_{52}$H$_{41}$NO$_3$P$_2$Cl$_2$Ru: C, 64.94; H, 4.30; N, 1.46. MS (ES$^+$, CH$_2$Cl$_2$, *m/z*): 964.00 (M + H)$^+$, 926.01 (M − Cl)$^+$. ^{1}H NMR (CDCl$_3$, δ): 7.91 (d, 1H, H(7), J_{HH} 12.1), 14.91 (d, 1H, N$^+$–H, J_{HH} 12.0), 6.67 (s, 1H, H(3)), 7.09 (s, 1H, H(5)), 2.08 (s, 3H, CH$_3$), 7.09–7.66 (m, 34H, 2PPh$_3$, H(11), H(12), H(14) and H(15), arom).

3.4. Synthesis of the complexes [Os(QL^3)(PPh$_3$)$_2$(CO)$_2$Br] (6)

The [Os(QL^3)(PPh$_3$)$_2$(CO)$_2$Br] (**6**) complexes were synthesized in excellent yield (~85%) by reacting [Os(QL^1)(PPh$_3$)$_2$(CO)Br] with carbon monoxide. Details of a representative case are given below.

3.4.1. [Os(MeL^3)(PPh$_3$)$_2$(CO)$_2$Br] (6(Me))

One hundred milligrams (0.099 mmol) of Os (MeL^1)(PPh$_3$)$_2$(CO)Br was treated with carbon monoxide in the same manner as in the case **5** (Me). Here the solution colour changed from violet to yellow after 6 h. After that solvent was evaporated under reduced pressure when a yellow solid was obtained which was treated with dichloromethane and petroleum ether (b.p. 60–80 °C) in the same manner as in the case of **5**

(Me). The yellow solid was finally dried in vacuo. Yield: 88 mg (85%). Anal. Found: C, 59.18; H, 4.05; N, 1.25%. Calc. for $C_{53}H_{44}NO_3P_2BrOs$: C, 59.22; H, 4.12; N, 1.30. MS (ES$^+$, CH_2Cl_2, m/z): 1076.08 (M + H)$^+$, 995.12 (M − Br)$^+$. ^{1}H NMR (CDCl$_3$, δ): 8.04 (s, 1H, H(7)), 13.18 (s, 1H, O–H), 6.48 (s,1H, H(3)), 1.72 and 2.40 (2s, 6H, 2CH$_3$), 7.03–7.56 (m, 35H, 2PPh$_3$, H(5), H(12), H(13), H(15) and H(16), arom).

3.4.2. $[Os(MeOL^3)(PPh_3)_2(CO)_2Br]$ (6(OMe))

One hundred milligrams (0.098 mmol) Os-(MeOL^1)(PPh$_3$)$_2$(CO)Br was employed. Yield: 91 mg (89%). Anal. Found: C, 58.28; H, 4.12; N, 1.35%. Calc. for $C_{53}H_{44}NO_4P_2BrOs$: C, 58.35; H, 4.06; N, 1.28. MS (ES$^+$, CH_2Cl_2, m/z): 1092.07 (M + H)$^+$, 1012.11(M − Br)$^+$. ^{1}H NMR (CDCl$_3$, δ): 8.04 (s, 1H, H(7)), 13.18 (s, 1H, O–H), 6.47 (s, 1H, H(3)), 1.72 (s, 3H, CH$_3$), 3.86 (s, 3H, OCH$_3$), 6.94–7.56 (m, 35H, 2PPh$_3$, H(5), H(12), H(13), H(15) and H(16), arom).

3.4.3. $[Os(ClL^3)(PPh_3)_2(CO)_2Br]$ (6(Cl))

One hundred milligrams (0.098 mmol) Os(ClL^1)(PPh$_3$)$_2$(CO)Br was employed. Yield: 88 mg (86%). Anal. Found: C, 57.10; H, 3.70; N, 1.21%. Calc. for $C_{52}H_{41}NO_3P_2ClBrOs$: C, 57.02; H, 3.77; N, 1.28. MS (ES$^+$, CH_2Cl_2, m/z): 1096.05 (M + H)$^+$, 1016.09 (M − Br)$^+$. ^{1}H NMR (CDCl$_3$, δ): 7.95 (s, 1H, H(7)), 12.81 (s, 1H, O–H), 6.42 (s, 1H, H(3)), 1.65 (s, 3H, CH$_3$), 7.01–7.41 (m, 35H, 2PPh$_3$, H(5), H(12), H(13), H(15) and H(16), arom).

3.5. X-ray structure determination

A bright orange single crystal of Ru(ClL^2)(PPh$_3$)$_2$-(CO)Cl, (5 (Cl)) (0.40 × 0.30 × 0.20 mm^3) grown by slow diffusion of hexane into dichloromethane solutions at room temperature was used. Cell parameters were determined by a least squares fit of 30 machine-centered reflections (2θ range 14–28°) on a Siemens R3m/V four-circle diffractometer with graphite-monochromated Mo Kα radiation ($\lambda = 0.71073$). Two check reflections measured after every 198 reflections showed no significant intensity reduction. All data were corrected for Lorentz polarization effects and an empirical absorption correction [25] was performed on the basis of an azimuthal scan of six reflections for the crystals. The metal atom was located from Patterson maps and the rest of the non-hydrogen atoms emerged from successive Fourier syntheses. The structure was refined by full matrix least-squares procedures. All non-hydrogen atoms were refined anisotropically. Many of the significant hydrogen atoms were located in difference Fourier maps and the others were added at calculated positions. Calculations were performed using the SHELXTL, version 5.03 [26] programme package. Significant crystal data are listed in Table 4.

Table 4
Crystal data for Ru(ClL^2)(PPh$_3$)$_2$(CO)Cl

Complex	Ru(ClL^2)(PPh$_3$)$_2$(CO)Cl
Empirical formula	$C_{52}H_{41}NO_3P_2Cl_2Ru$
Formula weight	961.77
Crystal system	Monoclinic
Space group	$C2/c$
a (Å)	34.322(7)
b (Å)	14.472(3)
c (Å)	22.554(5)
β (°)	105.28(3)
V (Å^3)	10,807(4)
Z	8
μ (Mo Kα) (mm^{-1})	0.485
D_{calc} (g cm^{-1})	1.182
Total reflections	8151
Independent reflections (R_{int})	8151 (0.0000)
R_1[a], wR_2[b] [$I > 2\sigma(I)$]	4.49, 13.53

[a] $R_1 = \sum \|F_o| - |F_c\| / \sum |F_o|$.
[b] $wR_2 = [\sum w(F_o^2 - F_c^2)^2 / \sum (F_o^2)^2]$.

4. Conclusion

It is demonstrated that the metallacycle **3** undergoes facile one-carbon expansion upon treatment with carbon monoxide furnishing the acyl complex **5** presumably via aryl migration in a dicarbonyl intermediate. In **5**(Cl) we have a new structurally characterized acylruthenium metallacycle. The reaction of **4** with carbon monoxide affords the dicarbonyl aryl complex **6** and its stability is consistent with the poor ability of osmium in promoting aryl migration. The distinctive spectral features of **5** and **6** concern MLCT transitions, C=N and C≡O stretching frequencies and ^{31}P NMR chemical shifts. The M^{III}/M^{II} reduction potentials follow the order **5** > **3** and **6** > **4** signifying stabilization of the M^{II} state upon carbonylation.

5. Supplementary material

Crystallographic data for the structure analysis have been deposited with the Cambridge Crystallographic Data Centre, CCDC no. 262182 corresponding to Ru(ClL^2)(PPh$_3$)$_2$(CO)Cl, (**5**(Cl)). Copies of this information may be obtained free of charge from The Director, CCDC, 12 Union Road, Cambridge CB2 1EZ, UK (Fax: +44 1223 336033; e-mail: deposit@ccdc.cam.ac.uk or http://www.ccdc.cam.ac.uk).

References

[1] (a) A.D. Kovacs, D.S. Marynick, J. Am. Chem. Soc. 122 (2000) 2078;
(b) S. Niu, M.B. Hall, Chem. Rev. 100 (2000) 353;
(c) F. Calderazzo, Angew. Chem. Int. Ed. Engl. 16 (1977) 299.

[2] (a) R.H. Crabtree, The Organometallic Chemistry of the Transition Metals, third ed., Wiley, New York, p. 174;
(b) J.P. Collman, L.S. Hegedus, J.R. Norton, R.G. Finke, Principles and Applications of Organotransition Metal Chemistry, University Science Books, Mill Valley, CA, 1987 (Chapter 12);
(c) J. Tsuji, Organic Syntheses by Means of Transition Metal Complexes, Springer, Berlin, 1975.

[3] (a) C.F. Barnard, J.A. Daniels, R.J. Mawby, J. Chem. Soc., Chem. Commun. (1976) 1032;
(b) C.F. Barnard, J.A. Daniels, R.J. Mawby, J. Chem. Soc. Dalton Trans. (1979) 1331;
(c) S.A. Chawdhury, Z. Dauter, R.J. Mawby, C.D. Reynolds, D.R. Saunders, M. Stephenson, R.J. Mawby, J. Chem. Soc. Dalton Trans. (1984) 1153.

[4] (a) G. Cardaci, G. Reichenbach, G. Bellachioma, Organometallics 7 (1988) 2475;
(b) M. Aubert, G. Bellachioma, G. Cardaci, A. Macchioni, G. Reichenbach, M.C. Burla, J. Chem. Soc., Dalton Trans. (1997) 1759.

[5] (a) K.R. Grundy, J. Jenkins, J. Organomet. Chem. 265 (1984) 77;
(b) T.W. Dekleva, B.R. James, J. Chem. Soc., Chem. Commun. (1983) 1350.

[6] (a) G.R. Clark, W.R. Roper, L.J. Wright, V.P.D. Yap, Organometallics 16 (1997) 5135;
(b) D.S. Bohle, G.R. Clark, C.E.F. Rickard, W.R. Roper, W.E.B. Shepard, L.J. Wright, J. Chem. Soc. Chem. Commun. (1987) 563;
(c) W.R. Roper, G.E. Taylor, J.M. Waters, L.J. Wright, J. Organomet. Chem. 182 (1979) C46;
(d) W.R. Roper, L.J. Wright, J. Organomet. Chem. 142 (1977) C1.

[7] J.F. Hartwig, R.G. Bergman, R.A. Andersen, J. Am. Chem. Soc. 113 (1991) 6499.

[8] M.A. Bennett, A.M. Clark, M. Contel, C.E.F. Rickard, W.R. Roper, L.J. Wright, J. Organomet. Chem. 601 (2000) 299.

[9] K.A. Johnson, W.L. Gladfelter, Organometallics 11 (1992) 2534.

[10] B.D. Rowsell, R. McDonald, M. Cowie, Organometallics 23 (2004) 3873.

[11] (a) K. Ghosh, S. Pattanayak, A. Chakravorty, Organometallics 17 (1998) 1956;
(b) K. Ghosh, S. Chattopadhyay, S. Pattanayak, A. Chakravorty, Organometallics 20 (2001) 1419;
(c) S. Chattopadhyay, K. Ghosh, S. Pattanayak, A. Chakravorty, J. Chem. Soc., Dalton Trans. (2001) 1259;
(d) S. Chattopadhyay, K. Ghosh, S. Pattanayak, A. Chakravorty, Indian J. Chem. A 40 (2001) 1.

[12] B.K. Panda, S. Chattopadhyay, K. Ghosh, A. Chakravorty, Organometallics 21 (2002) 2773.

[13] (a) P. Ghosh, A. Pramanik, A. Chakravorty, Organometallics 15 (1996) 4147;
(b) P. Ghosh, A. Chakravorty, Inorg. Chem. 36 (1997) 64;
(c) P. Ghosh, Polyhedron 16 (1997) 1343;
(d) B.K. Panda, J. Chem. Sci. 116 (2004) 245.

[14] (a) B.K. Panda, S. Chattopadhyay, K. Ghosh, A. Chakravorty, Polyhedron 21 (2002) 899;
(b) S. Chattopadhyay, B.K. Panda, K. Ghosh, A. Chakravorty, Israel J. Chem. 41 (2001) 139.

[15] (a) B.K. Panda, K. Ghosh, S. Chattopadhyay, A. Chakravorty, J. Organomet. Chem. 674 (2003) 107;
(b) B.K. Panda, S. Sengupta, A. Chakravorty, Eur. J. Inorg. Chem. (2004) 178.

[16] (a) N. Bag, S.B. Choudhury, G.K. Lahiri, A. Chakravorty, J. Chem. Soc., Chem. Commun. (1990) 1626;
(b) N. Bag, S.B. Choudhury, A. Pramanik, G.K. Lahiri, A. Chakravorty, Inorg. Chem. (1990) 5014.

[17] P. Ghosh, N. Bag, A. Chakravorty, Organometallics 15 (1996) 3042.

[18] N. Serpone, D.G. Bickley, Prog. Inorg. Chem. 17 (1972) 391.

[19] (a) C. Sandorfy, D. Vocelle, Mol. Phys. Chem. Biol. 4 (1989) 195;
(b) J. Favrot, D. Vocelle, C. Sandorfy, Photochem. Photobiol. 30 (1979) 417.

[20] H. Bohme, M. Haake, In: H. Bohme, H.G. Viehe (Eds.), Advances in Organic Chemistry, part 1, vol. 9, Interscience, New York, 1976, p.1.

[21] (a) C.E.F. Rickard, W.R. Roper, S.D. Woodgate, L.J. Wright, J. Organomet. Chem. 643 (2002) 168;
(b) F. Kong, W. Wong, J. Organomet. Chem. 589 (1999) 191;
(c) C.E.F. Rickard, W.R. Roper, G.R. Whittell, L.J. Wright, J. Organomet. Chem. 689 (2004) 605.

[22] T.A. Stephenson, G. Wilkinson, J. Inorg. Nucl. Chem. 28 (1966) 945.

[23] P.R. Hoffman, K.G. Caulton, J. Am. Chem. Soc. 99 (1975) 4221.

[24] (a) G.K. Lahiri, S. Bhattacharya, B.K. Ghosh, A. Chakravorty, Inorg. Chem. 26 (1987) 4324;
(b) D.T. Sawyer, J.L. Roberts Jr., Experimental Electrochemistry for Chemists, Wiley, New York, 1974, p. 167.

[25] A.C.T. North, D.C. Phillips, F.A. Mathews, Acta Crystallogr. Sect. A 24 (1968) 351.

[26] G.M. Sheldrick, SHELXTL, version 5.03; Siemens Analytical X-ray System Madison, WI, 1994.